*Geophys. J. Int.* (2003) **152,** 215–227

# Oceanic and atmospheric excitation of the Chandler wobble

Dechun Liao,[1,2] Xinhao Liao[1,2] and Yonghong Zhou[1,2]

[1] *Shanghai Astronomical Observatory, Chinese Academy of Sciences,* 80 *Nan Dan Rd, Shanghai* 200030, *China. E-mail: ldc@center.shao.ac.cn*
[2] *National Astronomical Observatories, Chinese Academy of Sciences, Beijing* 100012, *China*

Accepted 2002 July 30. Received 2002 July 15; in original form 2001 October 10

## SUMMARY

The excitation mechanism of the Chandler wobble (CW) is investigated by examining the power spectra of oceanic angular momentum (OAM) excitation (1985–1995) and two series of atmospheric angular momentum (AAM) excitation. The power spectra are then compared with those of the observed excitation derived from the polar motion of COMB2000 series for different periods of time. The results show that the excitation from OAM can provide approximately 64 per cent of the required energy of the observed CW excitation, while the energy from AAM excitation is comparable with that of the observed CW excitation sometimes, but it is far less than that of the observed one at other times. The multitaper coherence analysis method is also used to investigate the relationship between the observed CW excitation and the geophysical excitation derived from OAM and AAM in the frequency domain. The results show that there is a high coherence (0.52) between the OAM excitation and the observed one during 1985–1995, while large fluctuations of the coherence and linear trend of the coherent phases exist between the AAM excitation and the observed one during 1962–2000. Some analyses are also made concerning the effects of different CW periods and quality factor ($Q$) on the CW excitation.

**Key words:** atmospheric angular momentum, Chandler wobble, excitation mechanism, oceanic angular momentum, polar motion.

## 1 INTRODUCTION

Variation of the Earth's rotation includes changes of the rotation rate (or the length of the day) and slight movement of the rotation axis relative to the surface of the Earth, the later is usually referred to as the polar motion. One of the main components of the polar motion is the Chandler wobble (CW) with central frequency at approximately 0.843 cycle per year (cpy) and amplitude approximately 200 milliarcsecond (mas). The CW is a mode of free oscillation of the Earth. If there were no excitation sources, the CW would have vanished by damping. Since the CW was discovered in 1891, its period, amplitude and damping factor have been estimated by many authors (Munk & MacDonald 1960; Currie 1974; Wilson & Haubrich 1976; Smith & Dahlen 1981; Okubo 1982a,b; Dong 1986; Wilson & Vicente 1990; Zhu 1991, 1992; Gao 1993; Furuya *et al.* 1996; Kuehne *et al.* 1996; Vicente & Wilson 1997). As for the excitation sources, many authors have estimated contributions from the atmosphere (Wilson & Haubrich 1976; Wahr 1983; Furuya *et al.* 1996, 1997; Celaya *et al.* 1999; Aoyama & Naito 2001), continental water storage (Chao *et al.* 1987; Hinnov & Wilson 1987; Kuehne & Wilson 1991), and some other possible excitation sources such as earthquakes (Munk & MacDonald 1960; Lambeck 1980; Gross 1985, 1986; Gross & Chao 1985, 1990; Souriau & Cazenave 1985; Chao & Gross 1987; Gu 1996), core–mantle coupling (Gire & Le Mouel 1986; Hinderer *et al.* 1987; Jault & Le Mouel 1993) and oceanic processes (Ponte *et al.* 1998; Celaya *et al.* 1999; Chao & Zhou 1999; Gross 2000a), etc. Among these excitation mechanisms, the seismic excitation is found to have little effect on the Chandler wobble because their contributions are two to five orders of magnitude smaller than the required Chandler wobble excitation power (Souriau & Cazenave 1985; Gross 1986; Chao & Gross 1987). Though a number of studies suggest the possibility of CW excitation from core–mantle coupling (Le Mouel *et al.* 1985; Runcorn *et al.* 1988; Jault & Le Mouel 1993), so far there is little convincing observational evidence. The CW excitation from continental water storage is found to have a high correlation with the observed one. However, there are inconsistencies in the estimates of the excitation from continental water storage mainly because of different data sets and models used by different authors. The CW excitation from oceanic processes has been investigated during recent decades. The main difficulty is the lack of observation data of the worldwide ocean bottom pressures and currents. Thus, the estimate of the CW excitation depends, to a large extent, on the oceanic dynamic models. The CW excitation from the atmosphere has been investigated over a long time, and the main contribution is found to be the barometric pressure. However, the contribution from the wind term has recently been found to have significant effects on the CW excitation.

Furuya *et al.* (1996) analysed the atmospheric contribution to the CW excitation over approximately 11 yr beginning in 1983

September, and found that in the vicinity of the Chandler frequency the power of the AAM excitation was comparable to the observed one with the wind contribution being larger than the pressure contribution; Aoyama & Naito (2001) analysed the CW excitation of atmospheric wind and pressure variations using the AAM data of approximately 15 yr derived from the Japan Meteorological Agency (JMA), and found that variations of the wind term and the pressure term (with an inverted barometry (IB) assumption) maintain a major part of the observed CW. Gross (2000a) analysed the observed polar motion excitation and the excitation derived from AAM and OAM by fast Fourier transform (FFT) power spectral densities and found that during 1985–1995 the CW was primarily excited by a combination of atmospheric and oceanic processes with the dominant excitation mechanism being the ocean bottom-pressure fluctuations. However, the authors in the above-mentioned three papers used slightly short data series (11, 15 and 11 yr) of AAM and OAM. Nowadays much longer data series of accurate polar motion and AAM are available. This allows us to analyse a long excitation series (39 yr) of the AAM by calculating its power spectral density in the Chandler wobble band and comparing it with that of the observed excitation derived from geodetic data on polar motion. Furthermore, both Furuya *et al.* (1996) and Aoyama & Naito (2001) used a CW frequency of 0.847 cpy (or 431 mean solar days in period). Some discussions for the effects of choosing different CW periods and quality factors ($Q$) on the results of the CW excitation will be made in Section 4.

## 2 DATA USED IN THIS STUDY

The data on geodetic polar motion analysed in this study are from the COMB2000 series (Gross 2000b) for 1962–2000 in 5 d intervals, which was obtained from the Jet Propulsion Laboratory (JPL), USA. The data consist of the coordinates $(X, Y)$ and their variation rates $(dX, dY)$ of the north pole of the rotation axis of the Earth with respect to the pole of the Terrestrial Reference Frame.

The AAM function was first introduced by Barnes *et al.* (1983) when investigating the excitation of the variation of wind and barometric pressure on the Earth's rotation. Equatorial components $\chi_1$ and $\chi_2$ of the AAM function (pointing to 0° and 90°E, respectively) are involved in the polar motion excitation. Each of them consists of a wind term (a motion term) and a pressure term (a mass term), which are usually distinguished by the superscripts w and p, respectively. The components $(\chi_1, \chi_2)$, $(\chi_1^{\mathrm{w}}, \chi_2^{\mathrm{w}})$ and $(\chi_1^{\mathrm{p}}, \chi_2^{\mathrm{p}})$ form vectors $\chi$, $\chi^{\mathrm{w}}$ and $\chi^{\mathrm{p}}$ in the complex plane, respectively. These components and vectors can be expressed as follows:

$$\begin{aligned}
\chi &= \chi_1 + i\chi_2 \\
&= \left(\chi_1^{\mathrm{w}} + \chi_1^{\mathrm{p}}\right) + i\left(\chi_2^{\mathrm{w}} + \chi_2^{\mathrm{p}}\right) \\
&= \chi^{\mathrm{w}} + \chi^{\mathrm{p}}, \\
\chi^{\mathrm{w}} &= \chi_1^{\mathrm{w}} + i\chi_2^{\mathrm{w}} \\
&= \frac{1.5913\bar{R}^3}{g\Omega(C-A)} \int_{\phi_1}^{\phi_2}\int_{\lambda_1}^{\lambda_2}\int_{p_1}^{p_2} (u\sin\phi + iv)\cos\phi\, \mathrm{e}^{i\lambda} dp\, d\lambda\, d\phi, \\
\chi^{\mathrm{p}} &= \chi_1^{\mathrm{p}} + i\chi_2^{\mathrm{p}} \\
&= \frac{-1.0980\bar{R}^4}{g(C-A)} \int_{\phi_1}^{\phi_2}\int_{\lambda_1}^{\lambda_2} p_{\mathrm{s}} \sin\phi\cos^2\phi\, \mathrm{e}^{i\lambda}\, d\lambda\, d\phi,
\end{aligned} \tag{1}$$

where $p_{\mathrm{s}}$ is the atmospheric pressure on the Earth's surface, $u$ and $v$ are the eastward and northward wind velocities, $\lambda$ and $\phi$ are the longitude and latitude, $g$ is the acceleration due to gravity on the Earth's surface, $\bar{R}$ and $\Omega$ are the mean radius and mean rotation rate of the Earth, $C$ and $A$ are the Earth's axial and equatorial principal moments of inertia, respectively. Two numerical coefficients of 1.0980 and 1.5913 account for the effects of surface loading and rotational deformation of the Earth (Eubanks 1993).

The data of AAM analysed in this study are those computed from the National Center for Environmental Prediction (NCEP)/National Center for Atmospheric Research (NCAR) reanalysis project (Salstein *et al.* 1993) and JMA (Naito *et al.* 1987), and they are obtained from the Special Bureau for the Atmosphere (SBA) of the International Earth Rotation Service (IERS).

The AAM (NCEP) series covers the period of 1962–2000 in 6 h intervals. From the data the wind (up to 10 mb), pressure (with the IB assumption) and the wind + IB pressure terms are averaged to obtain the 5 d mean values.

The AAM (JMA) series covers 1984–1999 in intervals from 6 h to 1 d for different periods of time. Because of the different intervals and some gaps in the data, a spline interpolation method is used to obtain the 5 d mean values of the wind (10 mb), IB pressure and the wind + IB pressure terms.

The OAM series covers 1985–1995 in 5 d intervals (Ponte *et al.* 1998) and is obtained from the Special Bureau for the Oceans (SBO) of the IERS. The OAM series consists of the bottom pressure and current terms, which are also added together to form a total OAM term in our analysis.

## 3 POLAR MOTION EXCITATION SERIES AND COMPARISON

### 3.1 Geodetic observed excitation and geophysical derived excitation

In a linearized form of the Liouville equation, the relation of the polar motion and its excitation can be written as (Munk & MacDonald 1960; Lambeck 1980)

$$i\frac{\dot{m}}{\sigma_{\mathrm{c}}} + m = \psi, \tag{2}$$

where $m = x - iy$ describes polar motion in the complex plane, $\sigma_{\mathrm{c}} = 2\pi f_{\mathrm{c}}(1 + i/2Q)$ is the complex Chandler frequency, where $f_{\mathrm{c}}$ and $Q$ are the real Chandler frequency and the quality factor of the Earth, respectively, and $\psi$ is the excitation function. Choosing $f_{\mathrm{c}} = 0.8435$ cpy and $Q = 179$ (Wilson & Vicente 1990), and using $X$, $Y$, $dX$ and $dY$ in COMB2000 series the geodetic observed polar motion excitation series (observed excitation for simplicity) can be obtained from eq. (2). Because of the resonance at frequencies near $f_{\mathrm{c}}$, the observed CW excitation expands to a broad band, which is the so-called Chandler wobble band (CWB). In this paper all of our discussions focus on the quantities at frequency $f_{\mathrm{c}} = 0.8435$ cpy and/or their mean values in the CWB.

For the geophysical excitation derived from OAM and AAM (OAM/AAM excitation for simplicity), according to Barnes *et al.* (1983) we have

$$\begin{aligned}
\psi^{\mathrm{w}} &= \chi_1^{\mathrm{w}} + i\chi_2^{\mathrm{w}}, \\
\psi^{\mathrm{pib}} &= \chi_1^{\mathrm{pib}} + i\chi_2^{\mathrm{pib}}, \\
\psi_{\mathrm{aam}} &= \left(\chi_1^{\mathrm{w}} + \chi_1^{\mathrm{pib}}\right) + i\left(\chi_2^{\mathrm{w}} + \chi_2^{\mathrm{pib}}\right),
\end{aligned} \tag{3}$$

$$\begin{aligned}
\psi^{\mathrm{c}} &= \chi_1^{\mathrm{c}} + i\chi_2^{\mathrm{c}}, \\
\psi^{\mathrm{bp}} &= \chi_1^{\mathrm{bp}} + i\chi_2^{\mathrm{bp}}, \\
\psi_{\mathrm{oam}} &= \left(\chi_1^{\mathrm{c}} + \chi_1^{\mathrm{bp}}\right) + i\left(\chi_2^{\mathrm{c}} + \chi_2^{\mathrm{bp}}\right),
\end{aligned} \tag{4}$$

where superscripts w and pib distinguish the wind and the IB pressure terms of AAM, and c and bp, the current and bottom-pressure terms of the OAM, respectively.

### 3.2 Analysis of power spectral densities

First, the data on the observed excitation and geophysical excitation derived from OAM, AAM (NCEP) and AAM (JMA) during 1985–1995 are analysed using an $N$-point FFT to obtain their power spectral densities (psd). A Hanning window is used for the FFT analysis to reduce the errors in the psd. In order to reduce the spectral leakage of the forced annual wobble excitation to the CW, the seasonal components (annual and semi-annual terms) together with an offset and trend terms in all of these excitation series are removed before the FFT analysis. Fig. 1 shows the comparison of the psd for the observed excitation (thick solid line) with those of the geophysical excitation (thin lines) derived from OAM (A1), AAM (NCEP) (A2), AAM (JMA) (A3), OAM + AAM (NCEP) (A4, solid line) and OAM + AAM (JMA) (A4, dashed line) for ±3 cpy during 1985–1995. The psd is integrated over the CWB (0.75–0.92 cpy), which gives an estimate of the averaged energy in mas$^2$, and the results are listed in the first line of Table 1(A). In addition, a similar analysis has been performed for short pieces of the data series during 1987–1995 and 1990–1995, and the results are listed in the second and third lines of Table 1(A).

A1, A2, A3 and A4 in Fig. 1 and Table 1(A) show that the ratios of the averaged energies in CWB of the OAM, AAM (NCEP), OAM + AAM (NCEP), AAM (JMA) and OAM + AAM (JMA) excitation to the observed excitation during 1985–1995 are 64, 23, 106, 214 and 427 per cent, respectively. This implies that, though excitation of the oceanic processes can provide a large part of the energy for the observed excitation in CWB, the energy of the OAM and AAM (NCEP) excitation cannot be responsible alone for the observed CW excitation in the period concerned. However, the total energy (5.18 mas$^2$) of the combined excitation of the OAM + AAM (NCEP) is slightly larger than the energy of the observed one (4.90 mas$^2$). This indicates that the oceanic and atmospheric processes can jointly supply sufficient energy to excite the observed Chandler wobble with a major contribution from the oceans. Among the oceanic excitation the contributions from the current, bottom pressure and current + bottom pressure are approximately 0.11, 3.01 and 3.13 mas$^2$, respectively. Our estimates are slightly small in comparison with 0.12, 3.45 and 3.69 mas$^2$ from Gross (2000a), and the main difference appears in the contribution of the bottom pressure. Another noticeable feature seen from Fig. 1 and Table 1 is that the energy (10.50 mas$^2$) of AAM (JMA) is much stronger than that (1.11 mas$^2$) of AAM (NCEP), and is more than twice as much as that (4.90 mas$^2$) of the observed one. It is difficult to say which of the AAM (NCEP) and AAM (JMA) is better. Apparently, the energy of the AAM (JMA), especially that of its wind term, seems too strong (8.84 mas$^2$ of the wind term and 1.62 mas$^2$ of the IB pressure term of the AAM (JMA) in contrast with 0.31 and 1.39 mas$^2$ of the AAM (NCEP)). Our estimates of the contribution to CW excitation from the wind + pressure (IB) terms of the AAM (NCEP) and the pressure (IB) term of the AAM (JMA) are consistent with 10–25 per cent of the observed excitation in previous studies (see, e.g., Wilson & Haubrich 1976; Wahr 1983; Vondrak 1990; Eubanks 1993). The significant difference of the estimated energies between AAM (NCEP) and AAM (JMA) further confirms the analyses in Aoyama & Naito (2000, 2001) that there exist some systematic differences in AAM series owing to the data and models used by NCEP and JMA. Unfortunately, there are no more AAM series available from SBA for this period that can be used to examine which of the AAM contributions (in particular, the wind contributions) is more reliable. One further feature that can be seen from Table 1 is that the psd (or energy) of both the observed and the geophysical excitation change significantly when different pieces of the data series are analysed. The results mentioned above are only derived from the 11 yr and shorter data series. To understand more clearly the variable relationship between the observed and geophysical excitation, the analysis of much longer data series is necessary.

### 3.3 Analysis of squared coherence

Besides comparing the observed excitation with those derived from geophysical processes in terms of the power spectral density (or energy), coherence analysis is also an important method in revealing the relationship between the two excitation series in the frequency domain (Wilson & Haubrich 1976; Kuehne & Wilson 1991; Kuehne *et al.* 1993; Furuya *et al.* 1996). For two time-series $X(t)$ and $Y(t)$ ($t = 0, 1, 2, \ldots, n-1$), the squared coherence is estimated by

$$\Gamma^2_{xy}(f) = \frac{|S_{xy}(f)|^2}{S_{xx}S_{yy}}, \tag{5}$$

where $S_{xx}$ and $S_{yy}$ are the auto-power spectra of the time-series $X(t)$ and $Y(t)$, respectively, $S_{xy}$ is the cross-power spectrum between them, and the coherence phase is estimated by

$$\Phi_{xy}(f) = \tan^{-1}\frac{\mathrm{Im}[S_{xy}(f)]}{\mathrm{Re}[S_{xy}(f)]}, \tag{6}$$

where $\mathrm{Im}[S_{xy}(f)]$ and $\mathrm{Re}[S_{xy}(f)]$ are the imaginary and the real parts of $S_{xy}(f)$, respectively. Before computing $S_{xx}(f)$, $S_{yy}(f)$ and $S_{xy}(f)$ using a Fourier transform, seven $4\pi$ orthogonal eigentaper windows (Thomson 1982; Zhou *et al.* 1997, 1998; Liao & Greiner-Mai 1999; Aoyama & Naito 2001) are applied to all the data series of the observed and the geophysical excitation. Although they degrade the spectral resolution, the use of multitaper windows greatly reduces the spectral leakage and hence improves the reliability of the spectral estimations. The estimates of the squared coherence and coherent phases between the observed and geophysical excitation are shown in B1–B4 and C1–C4 in Fig. 1, respectively. In B1–B4, the 90 per cent (0.32), 95 per cent (0.39) and 99 per cent (0.54) confidence thresholds of the squared coherence estimations are also shown as horizontal lines.

From the B panels of Fig. 1 it can be seen that at $f_c$ (0.8435 cpy) the squared coherence between the observed polar motion excitation and the geophysical excitation derived from OAM, AAM (NCEP), OAM + AAM (NCEP), AAM (JMA) and OAM + AAM (JMA) is very high. The average of the estimated squared coherence and coherent phases in CWB for 1985–1995, 1987–1995 and 1990–1995 are made and the results are listed in the first, second and third lines of Table 1(B) and (C), respectively. From the table, one can see that the mean values of the squared coherence between the observed excitation and AAM (OAM) excitation are 0.32 (AAM (NCEP)), 0.37 (AAM (JMA)) and 0.52 (OAM), and they are over the 90, 90 and 95 per cent confidence thresholds, respectively, while those between the observed excitation and joint excitation of OAM + AAM are 0.63 (OAM + AAM (NCEP)) and 0.62 (OAM + AAM (JMA)), respectively, and both of them are over the 99 per cent confidence thresholds. The coherent phases indicate that the observed excitation has a leading angle of approximately 19° relative to the OAM excitation, while it has lagging angles of approximately 47° and 19°

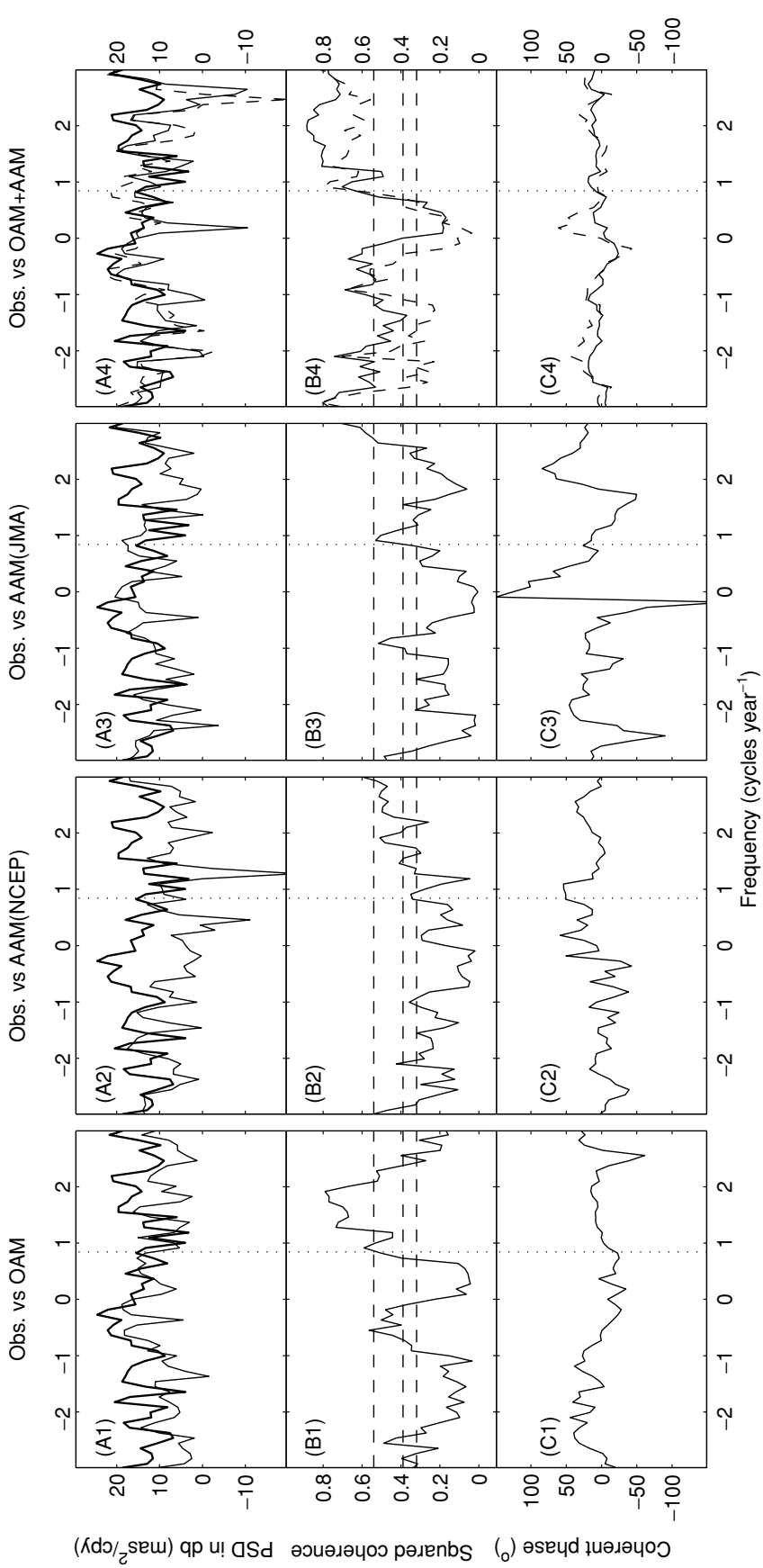


**Figure 1.** Comparison of the power spectral densities (A1–A4) of the observed excitation (thick solid line) with those geophysical excitation (thin lines) derived from OAM (left-hand box), AAM (NCEP) (mid-left), AAM (JMA) (mid-right), OAM + AAM (NCEP) (right, thin solid), and OAM + AAM (JMA) (right, thin dashed), the squared coherence (B1–B4) and coherent phases (C1–C4) between the observed and geophysical excitation for frequency range of ±3 cpy during 1985–1995. Three horizontal lines in B1–B4 show 90 per cent (0.32), 95 per cent (0.39) and 99 per cent (0.54) confidence thresholds of the squared coherence; the vertical line shows the CW frequency at 0.8435 cpy.

**Table 1.** Comparison of the mean values of the spectral energies (A, in mas$^2$) of the observed and geophysical excitation, squared coherence (B) and coherent phases (C, in deg) between the observed and geophysical excitation in the Chandler wobble band for different periods of time.

| Data | OBS | OAM | AAM (N) | OAM + AAM (N) | AAM (J) | OAM + AAM (J) |
|---|---|---|---|---|---|---|
| (A) Spectral power (mas$^2$) | | | | | | |
| 1985–1995 | 4.90 | 3.13 | 1.11 | 5.18 | 10.50 | 20.92 |
| 1987–1995 | 4.45 | 2.47 | 2.30 | 6.94 | 16.59 | 28.71 |
| 1990–1995 | 2.88 | 1.08 | 6.09 | 9.15 | 24.38 | 31.76 |
| 1962–2000 | 5.72 | – | 1.09 | – | – | – |
| (B) Squared coherence | | | | | | |
| 1985–1995 | – | 0.52 | 0.32 | 0.63 | 0.37 | 0.62 |
| 1987–1995 | – | 0.54 | 0.20 | 0.62 | 0.27 | 0.61 |
| 1990–1995 | – | 0.27 | 0.14 | 0.27 | 0.29 | 0.37 |
| 1962–2000 | – | – | 0.22 | – | – | – |
| (C) Coherent phases (deg) | | | | | | |
| 1985–1995 | – | −19.4 | 47.3 | 7.1 | 19.4 | 2.7 |
| 1987–1995 | – | −8.5 | 45.8 | 10.1 | 8.1 | 0.2 |
| 1990–1995 | – | −10.9 | 9.9 | 0.7 | 19.0 | 13.1 |
| 1962–2000 | – | – | 3.3 | – | – | – |

OBS, geodetic observed excitation.
AAM (N), excitation derived from AAM (NCEP) (wind + IB pressure).
OAM, excitation derived from ocean-bottom pressure + current.
OAM + AAM (N), excitation derived from OAM + AAM (NCEP).
AAM (J), excitation derived from AAM (JMA) (wind + IB pressure).
OAM + AAM (J), excitation derived from OAM + AAM (JMA).

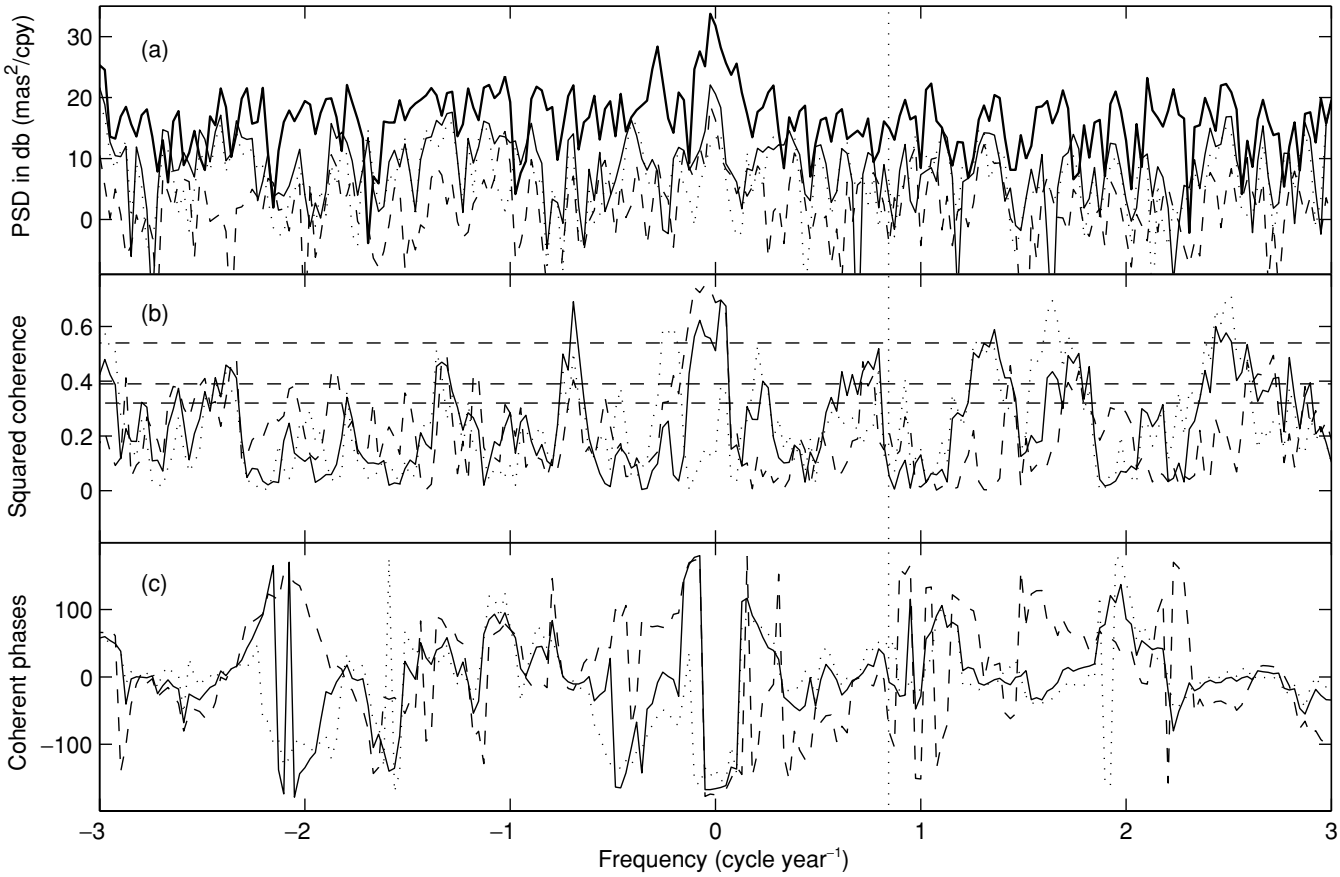


**Figure 2.** Same as in Fig. 1 but for the AAM (NCEP) during 1962–2000. The curves related to the wind, IB pressure and wind + IB pressure terms are shown in dashed, dotted and solid lines, respectively.

relative to the excitation of the AAM (NCEP) and AAM (JMA), respectively. That the leading angles of the OAM + AAM (NCEP) and OAM + AAM (JMA) excitation are approximately 7° and 3° relative to the observed one indicates that the joint excitation of OAM and AAM is more consistent with the observed one in phase than the OAM excitation or the AAM excitation is alone. However, the estimated coherence and coherent phases also change significantly for data series with a different duration.

### 3.4 Analysis of psd, squared coherence and coherent phase for longer data series

Both COMB2000 and AAM (NCEP) available for the time period 1962–2000 are used for further analysis. Using the observed excitation obtained from COMB2000 and geophysical excitation derived from the wind, IB pressure and wind + IB pressure terms of the AAM (NCEP) in Section 3.1, the psd of the observed and AAM excitation, the squared coherence and the coherent phases between them for the 39 yr period are shown in Fig. 2. The curves in the top panel show that the psd of the excitation from the wind, IB pressure and the wind + IB pressure terms for the frequency range from −3 to 3 cpy are, in most cases, much lower than that of the observed one. This indicates that the excitation energies from these atmospheric processes are far less than that of the observed excitation. The curves in the middle panel indicate that the estimates of the squared coherence between the observed and the AAM excitation in CWB are much lower than the 90 per cent confidence threshold. The mean energies of the observed excitation and the AAM (NCEP) excitation, and the mean coherence between the two excitations in CWB are also listed in Table 1. The mean energies of the observed and AAM excitation show no significant difference from the results for 1985–1995, but the coherence and coherent phase show some differences from those for 1985–1995.

In order to examine the above results in more detail, we perform an *N*-point FFT analysis and a multitaper coherent analysis for the 12 yr data, then we integrate the psd and average the squared coherence and coherent phases in the CWB, and finally, shift the data 3 months forward and repeat the same procedure until the end of the data series. The mean energies obtained for the observed CW excitation and the wind, IB pressure and wind + IB pressure excitation are shown by dotted, dashed, dot-dashed and solid lines in Fig. 3(a), the mean squared coherence and coherent phases in (b) and (c), respectively. Some results derived from AAM (JMA) during 1984–1999 are also shown in the figure as thin lines. Spanning only 11 yr of the OAM series, one value of the mean energy of the excitation is calculated and denoted in the figure by ○, and the value for

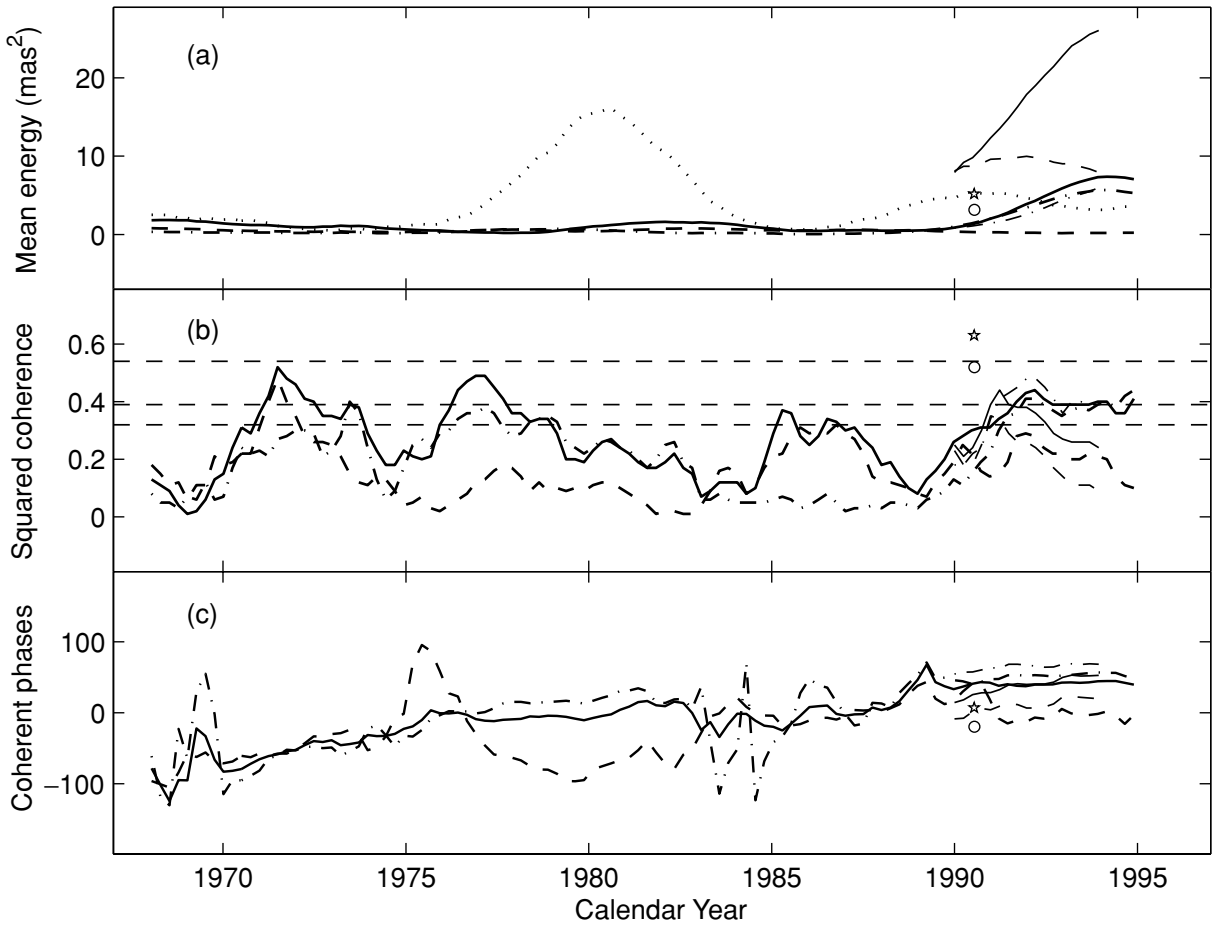


**Figure 3.** Temporal variations of: (a) the mean energies in CWB of the observed excitation (dotted line) and those of geophysical excitation derived from the AAM (NCEP) (denoted by thick lines) during 1962–2000, AAM (JMA) (by thin lines) during 1984–1999, OAM (by ○) during 1985–1995, and OAM + AAM (NCEP) (by a pentagram); (b) the squared coherence and (c) the coherent phases between the observed and geophysical excitation. The curves related to the wind, IB pressure and wind + IB pressure terms are shown in dashed, dash-dotted and solid lines, respectively. The three horizontal lines in (b) show the 90 per cent (0.32), 95 per cent (0.39) and 99 per cent (0.54) confidence thresholds of the coherence estimates.

**Table 2.** Summary of past and present estimates for the free Chandler wobble period and quality factor $Q$ and $1\sigma$ uncertainty (see Table 1 in Furuya & Chao 1996).

| No | Study | Period (d) | $Q$ (range) | Data (length in yr) |
|---|---|---|---|---|
| 1 | Jeffreys (1940) | $446.7 \pm 6.8$ | 46 (37, 60) | ILS (42) |
| 2 | Jeffreys (1968) | $433.2 \pm 3.4$ | 61 (37, 193) | ILS (68) |
| 3 | Wilson & Haubrich (1976) | $434.0 \pm 2.5$ | 100 (50, 400) | ILS (70) |
| 4 | Ooe (1978) | $434.8 \pm 2.0$ | 96 (50, 300) | ILS (76) |
| 5 | Wilson & Vicente (1980) | $433.3 \pm 3.6$ | 175 (48, 1000) | ILS (78) |
| 6 | Wilson & Vicente (1990) | $433.0 \pm 1.1$ | 179 (74, 789) | ILS + BIH (86) |
| 7 | Kuehne *et al.* (1996) | $439.5 \pm 1.2$ | – | Space93 + AAM (9) |
| 8 | Furuya & Chao (1996) | $433.7 \pm 1.8$ | 49 (35, 100) | Space94 + AAM (11) |

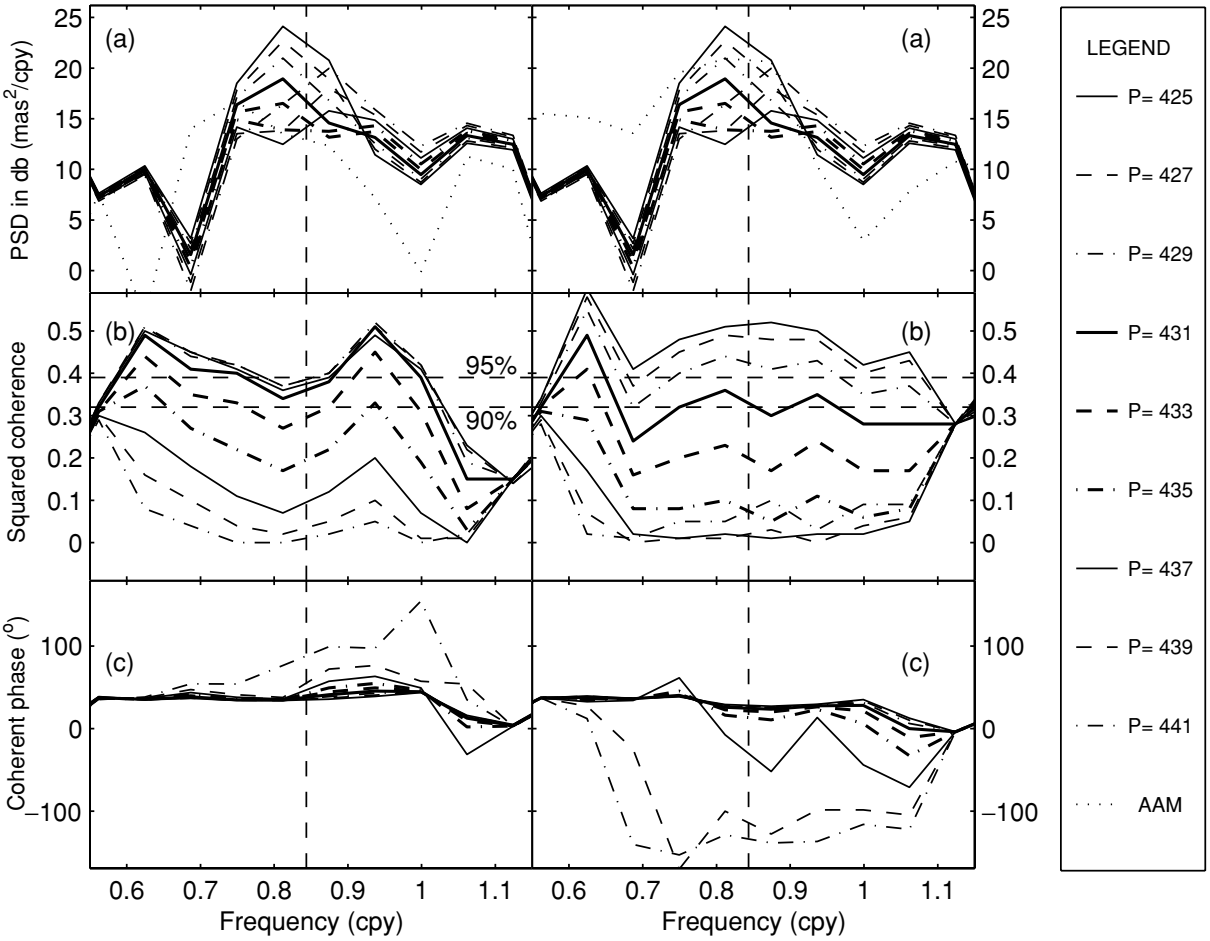


**Figure 4.** By setting $Q = 100$ and choosing different CW periods from 421 to 441 mean solar days, the power spectral density (a) of the observed excitation, the squared coherence (b) and the coherent phases (c) between the observed and geophysical excitation derived from AAM (NCEP) (left-hand panel) and AAM (JMA) (right-hand panel) in a frequency range of 0.55–1.15 cpy during 1984–1999. In (a), the psd of the AAM (NCEP) and AAM (JMA) excitation (both as a thin dotted line) are also shown, from which it is clear that the psd of the AAM (NCEP) excitation (left-hand panel) in the vicinity of 0.8435 cpy are lower than most of the observed ones calculated using different $p_c$; however, the psd of the AAM (JMA) excitation (right-hand panel) are larger than most of the observed ones. In (b), two horizontal lines show 90 and 95 per cent confidence thresholds for the estimates of the coherence. From (b) it can be seen that the two coherence values exceed the 90 per cent confidence threshold when $p_c = 431$ d, while the two coherence values are lower than the 90 per cent confidence threshold and the coherence between the observations and the AAM (JMA) excitation is lower than that between the observations and the AAM (NCEP) excitation when $p_c = 433$ d.

OAM + AAM (NCEP) denoted by $*$. From Fig. 3(a) one can clearly see the temporal variations of the mean energies in CWB of the observed excitation and the AAM excitation year by year. The fluctuation of the mean energies of the observed CW excitation is large over the whole period, while those of the AAM (NCEP) excitation are quite small except for the period after 1990. The excitation from the IB pressure and wind + IB pressure increase gradually and exceed the observed one after the middle of 1992, but the wind contribution remains at the same level as before. For 1975–1984 and 1986–1991, the mean energies of the AAM (NCEP) excitation are much less than those of the observed one. For instance, in the vicinity of 1980 the mean energies of the AAM excitation are less

than one 15th of the observed one. Secondly, in the panel the mean energies estimated from the wind, IB pressure and wind + IB pressure of the AAM excitation during 1990–1994 are approximately 0.24, 3.38, 3.92 mas$^2$ (NCEP) and 9.12, 2.94, 17.45 mas$^2$ (JMA), respectively. It can clearly be seen that the differences are mainly a result of the wind term. These results are similar to those of Aoyama & Naito (2001), where they analysed only 15 yr of data and calculated the mean energy using a 8 yr sliding window. Thirdly, the OAM excitation for 1985–1995 shows itself to be a major contribution in interpreting the observed CW excitation.

Shown by dashed, dash-dotted and solid lines, respectively, the curves in Fig. 3(b) clearly show the variation of the squared coherence between the observed excitation and the wind, IB pressure and wind + IB pressure of the AAM (NCEP) excitation. Most of the time these coherence values are lower than the 90 per cent confidence threshold, however, at some times, e.g. during 1971.2–1972.5, 1976.4–1977.7 and 1991.7–1994.2 the coherence between the observed excitation and the wind + IB pressure excitation exceeds the 95 per cent confidence threshold. The coherence between the observed excitation and the wind (or IB pressure) excitation are at slightly lower levels.

In Fig. 3(c) the coherent phases between the observed excitation and those derived from the IB pressure and the wind + IB pressure show steady linear variations (approximately 4 deg yr$^{-1}$ for both), while for the wind term, the coherent phases have a slightly slow variation rate (approximately 2.7 deg yr$^{-1}$). However, there are some times, e.g. in 1969, 1975 and 1984, when the coherent phases vary very quickly. We still do not have an explanation for these linear phase variations.

## 4 EFFECTS OF DIFFERENT CHANDLER WOBBLE PERIODS AND $Q$ ON ESTIMATES OF PSD, SQUARED COHERENCE AND COHERENT PHASES

As pointed out in Furuya *et al.* (1996), the assumed Chandler wobble period ($p_c$) is important in the comparison of the observed excitation and the geophysical excitation in the CWB. In this study, $f_c$ = 0.8435 cpy (or $p_c$ = 433.0 mean solar days) and $Q$ = 179 (Wilson & Vicente 1990) are chosen. This is because the $f_c$ is consistent with most of the $p_c$ estimates using geodetic observations. Here we recall Table 1 in Furuya & Chao (1996) which listed some typical values of $p_c$ and $Q$ estimated from 1940 to 1996 using 42–86 yr optical and 9–11 yr modern geodetic observations. Among the listed values of $p_c$, only the first one (estimated at early times and using short

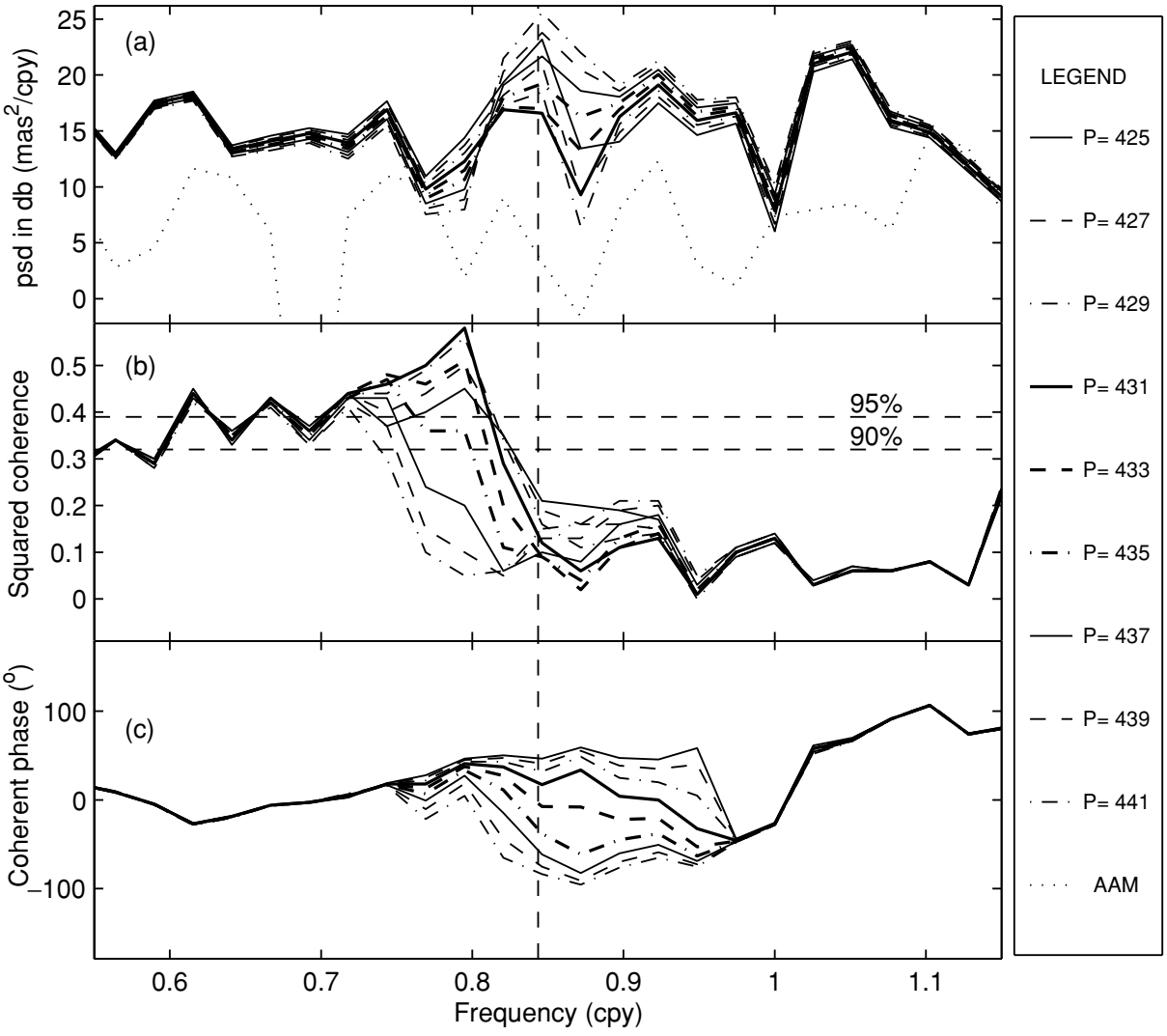


**Figure 5.** Same as in Fig. 4 but for AAM (NCEP) excitation during 1962–2000.

ILS data) and the seventh (using a short data version of the modern geodetic observations) are significantly different from the others. The average of the other six $p_c$ estimates is 433.7 d, and the average of $Q$ values in Table 2 is 100.9.

A comparison is made to examine the effects on the estimates of the CW excitation using different $p_c$ values from 421 to 441 d and different $Q$ from 50 to 250. First, by setting $Q = 100$ and changing the $p_c$ value from 421 to 441 d by every 2 d, the observed polar motion excitation is calculated according to eq. (2). In each case a power spectral analysis of the observed excitation and a multitaper coherence analysis between the observed excitation and the AAM excitation (from both NCEP and JMA) are made for the period 1984–1999 using the same methods as described in Section 3. Fig. 4 shows the estimates of the psd (a) of the observed excitation and AAM excitation, the estimates of squared coherence (b) and coherent phases (c) between the observed excitation and the AAM excitation for $p_c$ of 425–441 d in the frequency range 0.55–1.15 cpy (corresponding results for $p_c$ of 421 and 423 d are not shown in the figure to avoid using overly complex line styles).

As shown clearly in Fig. 4, different choices of $p_c$ cause large differences in estimates of the psd of the observed excitation, and in estimates of the squared coherence and the coherent phases between the observed and the AAM excitation during 1984–1999. At $f_c = 0.8435$ cpy, the ratio of the largest psd estimate of the observed excitation (322.5 mas$^2$ cpy$^{-1}$ for $p_c = 421$ d, not shown in Fig. 4a) to the smallest one (24.2 mas$^2$ cpy$^{-1}$ for $p_c = 435$ d) is approximately 13.3. The psd estimate for $p_c = 431$ d is approximately 1.6 times that for $p_c = 433$ d. From Fig. 4(a), one can also see that the psd estimates of the AAM (NCEP) and AAM (JMA) excitation are 19.5 mas$^2$ cpy$^{-1}$ (left) and 119.8 mas$^2$ cpy$^{-1}$ (right), respectively. The latter is approximately five times larger than the former.

Comparing the left and right groups of the curves in Fig. 4(b), we can see that the squared coherence can vary from approximately 0 to 0.4 between the observed and AAM (NCEP) excitation and from 0 to 0.5 between the observed and AAM (JMA) when choosing different values for $p_c$. For a given $p_c$ the coherence in the two group curves is considerably different. For example, by choosing $p_c = 433$ d, the estimates of the squared coherence at 0.8435 cpy are 0.30 (left) and 0.20 (right), respectively; while by choosing $p_c = 431$ d, the estimates of the coherence are 0.36 (left) and 0.33 (right), respectively.

As for the coherent phases in Fig. 4(c), when choosing $p_c$ from 421 to 435 d, the two groups of curves show average leading phases of approximately $36.8^\circ \pm 2.8^\circ$ for AAM (NCEP) and $27.8^\circ \pm 3.4^\circ$

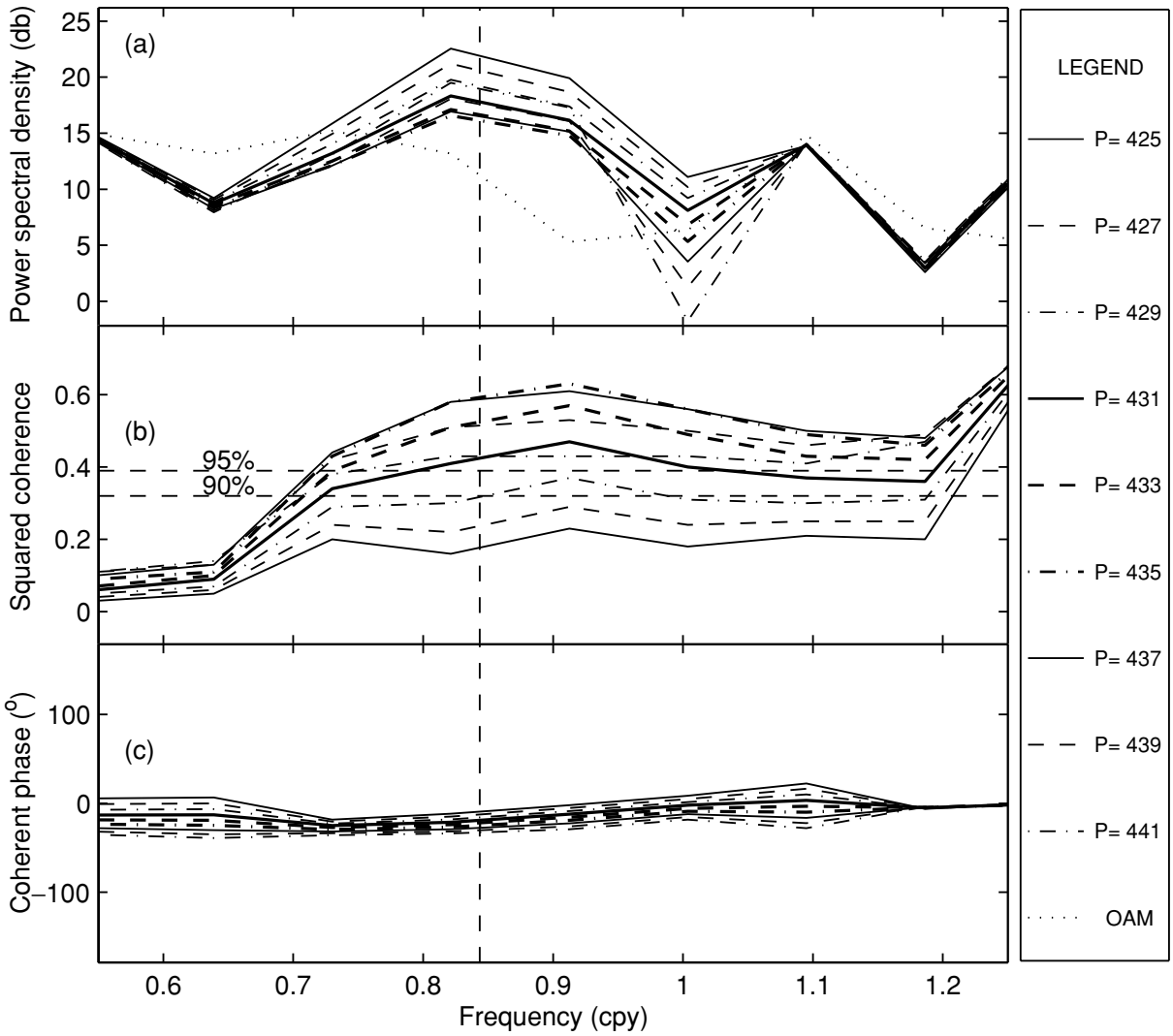


**Figure 6.** Same as in Fig. 4, but for OAM excitation during 1985–1995.

for AAM (JMA) relative to the phase of the observed excitation, but when choosing higher $p_c$ (e.g. 437–441 d), the coherent phases become larger.

The same analyses are also performed for longer data series of the observed excitation and AAM (NCEP) excitation during 1962–2000 and for the shorter data series of the observed excitation and OAM excitation during 1985–1995, and the results are displayed in Figs 5 and 6, respectively. Because of the different $p_c$ values used, large effects on the estimates of psd, coherence and coherent phases are shown in the two figures. In Fig. 5(a), the psd estimates of the observed excitation at $f_c$ vary from approximately 45.8 mas$^2$ cpy$^{-1}$ ($p_c = 431$ d) to 410.5 mas$^2$ cpy$^{-1}$ ($p_c = 421$ d), the latter is approximately nine times the former. When choosing $p_c$ as 431 and 433 d, the ratio of the psd estimates for the former to that for the latter is approximately 0.9. Another remarkable feature in Fig. 5(a) is that the psd estimate of the AAM (NCEP) excitation is only 2.4 mas$^2$ cpy$^{-1}$ (or 3.8 dB), approximately 1/20 of the psd of the geodetic CW excitation when choosing $p_c = 433$ d for 1962–2000, in contrast with 19.5 mas$^2$ cpy$^{-1}$ (or 12.9 dB), approximately 64 per cent of the psd of the geodetic CW excitation in Fig. 4(a) for 1984–1999. This again implies that the contribution of the AAM excitation on the CW excitation is temporarily unstable.

In Fig. 5(b), the squared coherence between the observed excitation and the AAM (NCEP) excitation vary from 0.09 for $p_c = 435$ d to 0.24 for $p_c = 421$ d, and all of them are far below the 90 per cent confidence threshold. When choosing $p_c$ as 431 and 433 d, the squared coherence values are 0.14 and 0.10, respectively, in contrast with 0.36 and 0.30 in the left-hand panel of Fig. 4(b) for 1984–1999. And from Fig. 5(c), the coherent phases at $f_c$ for different $p_c$ scatter to a larger range from approximately $-89^\circ$ ($p_c = 441$ d) to $53^\circ$ ($p_c = 421$ d) in contrast with a small range of $34^\circ$–$88^\circ$ in the left-hand panel of Fig. 4(c).

As in Figs 4 and 5, the effects of different $p_c$ on the estimates of psd for the observed excitation, the estimates of squared coherence and coherent phases between the observed excitation and OAM excitation during 1985–1995 are shown in Fig. 6. Some different features in Fig. 6 are as follows. First, the range of the variable psd (41.0–263.1 mas$^2$ cpy$^{-1}$) for the observed excitation in (a) becomes smaller than that in Fig. 4(a) (24.2–322.5 mas$^2$ cpy$^{-1}$ during 1984–1999) and Fig. 5(a) (45.8–410.5 mas$^2$ cpy$^{-1}$ during 1962–2000).

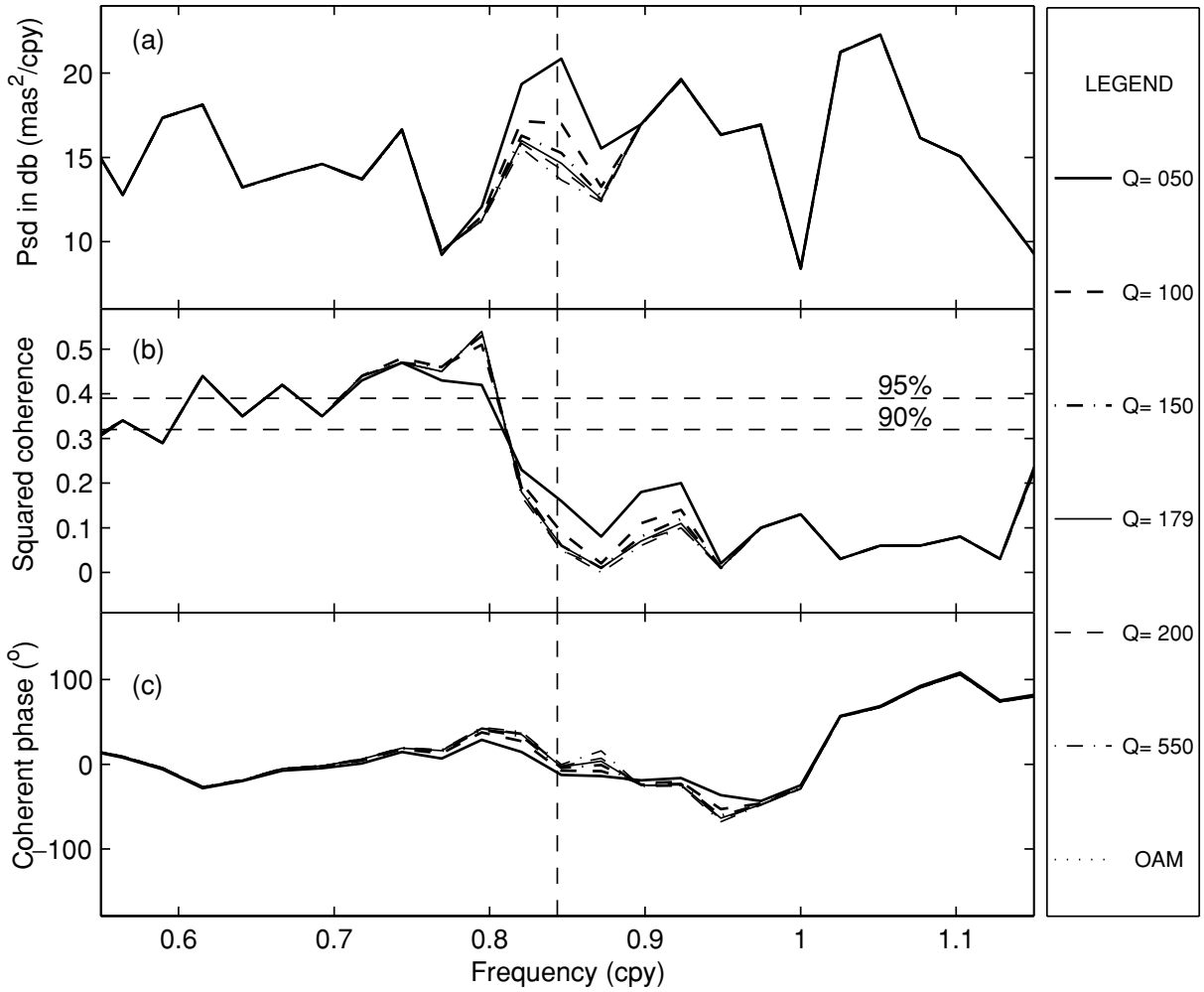


**Figure 7.** By setting $p_c = 433$ d and choosing different $Q$ values from 50 to 250, the power spectral density of the observed and AAM (NCEP) excitation (a), the squared coherence (b) and the coherent phases (c) between the observed and AAM (NCEP) excitation during 1962–2000. In (a), in the vicinity of a 0.8435 cpy difference of the psd of the observed excitation for $Q = 50$ is the largest one ($Q = 100$ gives the second largest), as do those for coherence and coherent phases between the observed and AAM (NCEP) excitation in (b) and (c) for $Q = 50$. Differences in psd, coherence and coherent phase for other $Q$ values are rather small.

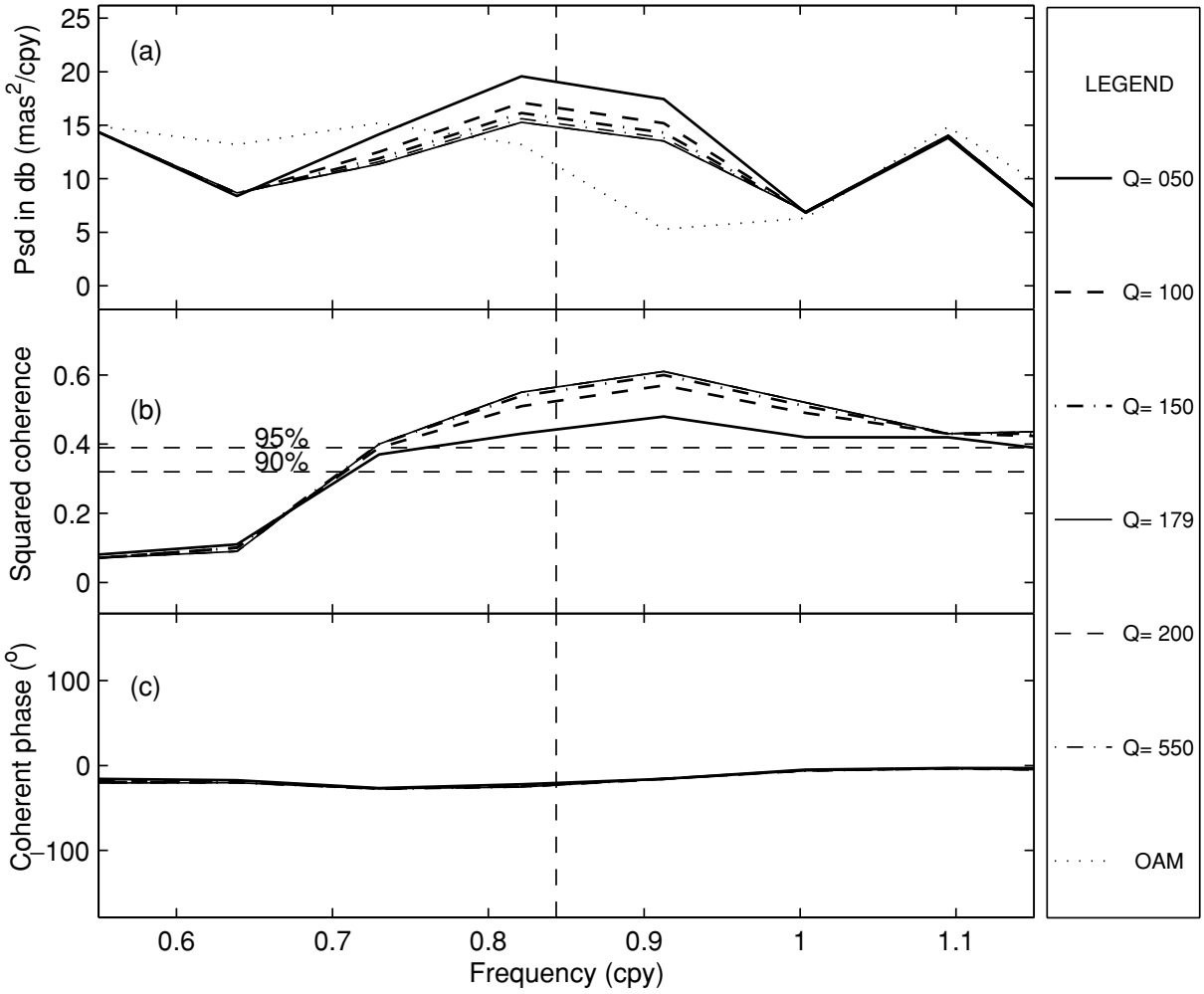


**Figure 8.** Same as in Fig. 7 but for OAM excitation during 1985–1995.

Secondly, the squared coherence between the observed and OAM excitation all exceed the 95 per cent confidence threshold when using a $p_c$ value of 431–441 d, among them the squared coherence is 0.42 and 0.52 for $p_c$ values of 431 and 433 d, respectively. However, when using $p_c$ values of 421–429 d, the squared coherence values between them are all below the 90 per cent confidence threshold. Thirdly, coherent phases between the observed excitation and the OAM excitation converge to a small range of $-2.5^\circ$ to $-35.5^\circ$ for different $p_c$. When choosing $p_c = 433$ d, the coherent phase is approximately $-23.9^\circ$ in contrast with $-19.4^\circ$ in Table 1 using the same $p_c$ but different $Q$ (=179).

By setting $p_c = 433$ d, Figs 7 and 8 show the effects of different $Q$ values on estimates of the psd of the observed excitation and on estimates of squared coherence and coherent phases between the observed excitation and AAM (NCEP) excitation during 1962–2000 and those between the observed and the OAM excitation during 1985–1995, respectively. The results in the two figures indicate that the effects arising from using different $Q$ values on the psd estimate of the observed excitation and on estimates of squared coherence and coherent phases between the observed excitation and AAM (OAM) excitation are also obvious, especially when using small $Q$. Gross (2000a) has discussed some effects by fixing $p_c = 433$ d and changing $Q$ from 179 to 74 and 138, and found the observed excitation power (integrated in a range of 0.730–0.913 cpy) to change from 4.87 mas$^2$ to 7.99 and 5.45 mas$^2$, respectively. In our case, the observed excitation power (integrated in a range of 0.75–0.92 cpy) changes from 4.92 mas$^2$ to 7.94 and 5.51 mas$^2$, respectively. Our results are in good agreement with those in Gross (2000a). Though the effects arising from the different $Q$ values are relatively small in comparison with the effects arising from using different $p_c$ values, the choice of $Q$ should also be considered.

## 5 CONCLUSION AND DISCUSSION

Our analysis shows that in the Chandler wobble band the OAM excitation can provide a large part of the energy to excite the Chandler wobble, the OAM + AAM (NCEP) excitation can completely explain the observed CW excitation, and both the OAM excitation and the joint excitation of the OAM + AAM (NCEP) have a high squared coherence with the observed CW excitation during 1985–1995. These further confirm the results in Gross (2000a). However, comparisons of the relationship between the observed excitation and the OAM excitation over shorter data series and between the observed excitation and the AAM excitation over longer data series indicate that the relationship is temporally variable. Though the OAM plays an important role in exciting the observed Chandler wobble during 1985–1995, estimating the OAM contribution more precisely over a long period is desirable.

We have noticed that a period of $p_c = 431$ d was chosen in Furuya *et al.* (1996), Furuya *et al.* (1997) and Aoyama & Naito (2000, 2001)

based on the closest agreement of the observed CW excitation with the AAM excitation. Because of the variable features of both the observed excitation and the AAM excitation, the $p_c$ value chosen in this way is also variable. For example, although our analysis of the relationship of the psd (at 0.8435 cpy) between the observed excitation and AAM (NCEP) excitation (see Fig. 5a) during 1962–2000 supports the optimal value of $p_c = 431$ d, the same analysis for data during 1984–1999 shows an optimal value of $p_c = 435$ d (see the left-hand side in Fig. 4 a), and the analysis of the observed excitation and the AAM (JMA) during 1984–1999 shows an optimal value of $p_c = 427$ d (right-hand panel in Fig. 4a). These values of $p_c$ are inconsistent with each other. So, the choice of CW period is still an open and sensitive topic and requires further attention.

As shown in Furuya *et al.* (1997), Aoyama & Naito (2000, 2001) and our analysis, the difference of the wind contribution of the CW excitation of AAM (NCEP) from AAM (JMA) raises another question: which of the wind contributions of the CW excitation is more reliable? We hope the problem of the discrepancy in wind excitation of the two AAM series will be solved as soon as possible to allow a better understanding of the mechanism of CW excitation.

## ACKNOWLEDGMENTS

We are grateful to Professor R. S. Gross for providing the JPL combined EOP 2000 series, to Gross and another anonymous referee for their valuable remarks, to NCEP/NCAR, JMA, SBA and SBO for their AAM and OAM data series. This work was supported by the Major project of the National Natural Scientific Foundation of China (NNSFC) (10133010), NNSFC (19833030, 19973011), and Shanghai Science and Technology Development Foundation (JC14012).

## REFERENCES

Aoyama, Y. & Naito, I., 2000. Wind contributions to the Earth's angular momentum budgets in seasonal variation, *J. geophys. Res.,* **105,** 12 417–12 431.

Aoyama, Y. & Naito I., 2001. Atmospheric excitation of the Chandler wobble, *J. geophys. Res.,* **106,** 8941–8954.

Barnes, R.T.H., Hide, R., White, A.A. & Wilson, C.R., 1983. Atmospheric angular momentum functions, length-of-day changes and polar motion, *Proc. R. Soc. Lond.*, A, **387,** 31–73.

Celaya, M.A., Wahr, M. & Bryan, F.O., 1999. Climate driven polar motion, *J. geophys. Res.,* **104,** 12 813–12 829.

Chao, B.F., Gross, R.S., 1987. Changes in the Earth's rotation and low-degree gravitational field induced by earthquakes, *Geophys. J. R. astr. Soc.,* **91,** 569–596.

Chao, B.F. & Zhou, Y.-H., 1999. Meteorological excitation of interannual polar motion by the North Atlantic Oscillation, *Geodynamics,* **27,** 61–73.

Chao, B.F., O'Connor, W.P., Chang, A.T.C., Hall, D.K. & Foster, J.L., 1987. Snow load effect on the Earth's rotation and gravitational field, 1979–1985, *J. geophys. Res.,* **92,** 9415–9422.

Currie, R.G., 1974. Period and $Q$ of the Chandler wobble, *Geophys. J.,* **38,** 179–185.

Dong, D.N., 1986. Measurement of the quality factor $Q$ of the Chandler wobble, *Acta Astr. Sinica,* **27,** 16–22.

Eubanks, T.M., 1993. Variations in the orientation of the Earth, in *Contributions of Space Geodesy to Geodynamics: Earth Dynamics, Geodyn. Ser.,* Vol. 24, pp. 1–54, eds Smith, D.E. & Turcotte, D.L., AGU, Washington, DC.

Furuya, M.Y. & Chao, B.F., 1996. Estimation of period and $Q$ of the Chandler wobble, *Geophys. J. Int.* **127,** 693–702.

Furuya, M., Hamano, Y. & Naito, I., 1996. Quasi-periodic wind signal as a possible excitation of Chandler wobble, *J. geophys. Res.,* **101,** 25 537–25 546.

Furuya, M., Hamano, Y. & Naito, I., 1997. Importance of wind for the excitation of Chandler wobble as inferred from wobble domain analysis, *J. Phys. Earth,* **45,** 177–188.

Gao, B.X., 1993. Is the Chandler period stable, *Sci. China,* **23,** 553–560.

Gire, C. & Le Mouel, J.-L., 1986. Flow in the fluid core and Earth's rotation, in *Earth Rotation: Solved and Unsolved Problems,* pp. 241–258, ed. Cazenave, A., Reidel, Dordrecht.

Gross, R.S., 1985. Signal detection techniques applied to the Chandler wobble, *J. geophys. Res.,* **90,** 10 281–10 290.

Gross, R.S., 1986. The influence of earthquake on the Chandler wobble during 1977–1983, *Geophys. J. R. astr. Soc.,* **85,** 161–177.

Gross, R.S., 2000a. The excitation of the Chandler wobble, *Geophys. Res. Lett.,* **27,** 2329–2332.

Gross, R.S., 2000b. Combinations of Earth orientation measurements: SPACE97, COMB97, and POLE97, *J. Geodesy,* **73,** 627–637.

Gross, R.S. & Chao, B.F., 1985. Excitation study of the LAGEOS-derived Chandler wobble, *J. geophys. Res.,* **90,** 9369–9380.

Gross, R.S. & Chao, B.F., 1990. The global geodynamic effect of the Macquaries Ridge earthquake, *Geophys. Res. Lett.,* **17,** 1009–1012.

Gu, Z-N., 1996. The study of excitation of the earthquake to earth's rotation, *Earth, Moon Planets,* **74,** 35–47.

Hinderer, J., Legros, H., Gire, C. & Le Mouel, J-L., 1987. Geomagnetic secular variation, core motions and implications for the Earth's wobble, *Phys. Earth planet. Inter.,* **49,** 121–132.

Hinnov, L.A. & Wilson, C.R., 1987. An estimate of the water storage contribution to the excitation of the polar motion, *Geophys. J. R. astr. Soc.,* **88,** 437–459.

Jault, D. & Le Mouel, J.-L., 1993. Circulation in the liquid core and coupling with the mantle, in *Observations of Earth from Space,* Vol. 13, p. 233, eds Singh, R.P., Feissel, M., Tapley, B.D. & Shum, C.K., *Adv. Space Res.,* Pergamon, Oxford.

Jeffeys, H., 1940. The variation of latitude, *Mon. Not. R. Astr. Soc.,* **100,** 139–155.

Jeffeys, H., 1968. The variation of latitude, *Mon. Not. R. Astr. Soc.,* **141,** 255–268.

Kuehne, J. & Wilson, C.R., 1991. Terrestrial water storage and polar motion, *J. geophys. Res.,* **96,** 4337–4345.

Kuehne, J., Johnson, S. & Wilson, C.R., 1993. Atmospheric excitation of nonseasonal polar motion, *J. geophys. Res.,* **98,** 19 973–19 978.

Kuehne, J., Wilson, C.R. & Johnson, S., 1996. Estimates of the Chandler wobble frequency and $Q$, *J. geophys. Res.,* **101,** 13 573–13 579.

Lambeck, K., 1980. *The Earth's Variable Rotation*, Cambridge University Press, New York.

Le Mouel, J.L., Gire, C. & Hinderer, J., 1985. Sur l'excitation possible de l'oscillation Chandlerienne par les mouvements a la surface du noyau, *C.R. Acad. Sci. Paris,* **301,** 27–32.

Liao, D.C., Greiner-Mai, H., 1999. A new $\Delta$LOD series in monthly intervals (1892.0–1997.0) and its comparison with other geophysical results, *J. Geodesy,* **73,** 466–477.

Munk, W.H. & MacDonald, G.J.F., 1960. *The Rotation of the Earth*,Cambridge University Press, New York.

Naito, I., Kikuchi, N. & Yokoyama, K., 1987. Results of estimating the atmospheric effective angular momentum functions based on the JMA global analysis data, *Pbl. Int. Latitude Obs. Mizusawa,* **20,** 1–11.

Okubo, S., 1982a. Is the Chandler period variable?, *Geophys. J. R. astr. Soc.,* **71,** 629–646.

Okubo, S., 1982b. Theoretical and observed $Q$ of the Chandler wobble—Love number approach, *Geophys. J. R. astr. Soc.,* **71,** 647–657.

Ooe, M., 1978. An optimal complex ARMA model of the chandler wobble, *Geophys. J.,* **53,** 445–457.

Ponte, R.M., Stammer, D. & Marshall, J., 1998. Oceanic signals in observed motions of the Earth pole of rotation, *Nature,* **391,** 476–479.

Runcorn, S.K. *et al.*, 1988. The excitation of the Chandler wobble, *Surv. Geophys.,* **9,** 419–449.

Salstein, D.A., Kann, D.M., Miller, A.J. & Rosen, R.D., 1993. The Sub-Bureau for Atmospheric Angular Momentum of the International Earth

Rotation Service: a meteorological data center with geodetic applications, *Bull. Amer. Meteor. Soc.,* **74,** 67–80.

Smith, M.L. & Dahlen, F.A., 1981. The period and *Q* of the Chandler wobble, *Geophys. J. R. astr. Soc.,* **64,** 223–281.

Souriau, A. & Cazenave, A., 1985. Reevaluation of the Chandler wobble seismic excitation from recent data, *Earth planet. Sci. Lett.,* **75,** 410–416.

Thomson, D.J., 1982. Spectrum estimation and harmonic analysis, *Proc. IEEE,* **70,** 1055–1096.

Vicente, R.O. & Wilson, C.R., 1997. On the variability of the Chandler frequency, *J. geophys. Res.,* **102,** 20 439–20 445.

Vondrak, J., 1990. Atmospheric and groundwater excitation of polar motion in case of variable Chandler frequency, *Bull. Astron. Inst. Czechosl.,* **41,** 211–220.

Wahr, J., 1983. The effects of the atmosphere and oceans on the Earth's wobble and on the seasonal variations in the length of day, II. results, *Geophys. J. R. astr. Soc.,* **74,** 451–487.

Wilson, C.R. & Haubrich, R.A., 1976. Meteorological excitation of the Earth's Wobble, *Geophys. J.,* **46,** 707–744.

Wilson, C.R. & Vicente, R.O., 1980. An analysis of the homogeneous ILS polar motion series, *Geophys. J. R. astr. Soc.,* **62,** 605–616.

Wilson, C.R. & Vicente, R.O., 1990. Maximum likelihood estimates of polar motion parameters, in *Variations in Earth Rotation,* eds McCarthy, D.D. & Carter, W.E., *Am. Geophys. Un. Geophys Monogr. Series,* Washington, DC.

Zhou, Y., Zheng, D., Zhao, M. & Chao, B.F., 1997. Polar motion and the North Atlantic Oscillation, *Chinese Sci Bull.,* **42,** 927–930.

Zhou, Y., Zheng, D., Zhao, M. & Chao, B.F., 1998. Interannual polar motion with relation to the North Atlantic Oscillation, *Global and Planetary Change, WE.,* **18,** 79–84.

Zhu, Y.Z., 1991. Theoretical period and *Q* of the Chandler wobble, *Sci. China, W.E.,* **21,** 1335–1340.

Zhu, Y.Z., 1992. The equilibrium pole tide of the anelastic earth and its effect on the Chandler wobble, *Acta Astr. Sinica,* **33,** 420–426.